Hindawi
Shock and Vibration
Volume 2024, Article ID 9802976, 1 page
https://doi.org/10.1155/2024/9802976

Retraction

Retracted: Study on Dynamic Evolution of Overburden Rock Movement and Mining-Induced Stress of Ultra-high Working Face

Shock and Vibration

Received 23 January 2024; Accepted 23 January 2024; Published 24 January 2024

This article has been retracted by Hindawi following an investigation undertaken by the publisher [1]. This investigation has uncovered evidence of one or more of the following indicators of systematic manipulation of the publication process:

(1) Discrepancies in scope

(2) Discrepancies in the description of the research reported

(3) Discrepancies between the availability of data and the research described

(4) Inappropriate citations

(5) Incoherent, meaningless and/or irrelevant content included in the article

(6) Manipulated or compromised peer review

The presence of these indicators undermines our confidence in the integrity of the article's content and we cannot, therefore, vouch for its reliability. Please note that this notice is intended solely to alert readers that the content of this article is unreliable. We have not investigated whether authors were aware of or involved in the systematic manipulation of the publication process.

Wiley and Hindawi regrets that the usual quality checks did not identify these issues before publication and have since put additional measures in place to safeguard research integrity.

We wish to credit our own Research Integrity and Research Publishing teams and anonymous and named external researchers and research integrity experts for contributing to this investigation.

The corresponding author, as the representative of all authors, has been given the opportunity to register their agreement or disagreement to this retraction. We have kept a record of any response received.

References

[1] T. Li, Z. Li, and J. Sun, "Study on Dynamic Evolution of Overburden Rock Movement and Mining-Induced Stress of Ultra-high Working Face," *Shock and Vibration*, vol. 2022, Article ID 2271635, 10 pages, 2022.

Hindawi
Shock and Vibration
Volume 2022, Article ID 2271635, 10 pages
https://doi.org/10.1155/2022/2271635

Research Article

Study on Dynamic Evolution of Overburden Rock Movement and Mining-Induced Stress of Ultra-high Working Face

Tao Li,[1,2] **Zheng Li**,[2] **and Jingdan Sun**[1]

[1]*Department of Resource Engineering, Heilongjiang University of Technology, Jixi 158100, China*
[2]*School of Energy and Mining Engineering, China University of Mining and Technology-Beijing, Beijing 100083, China*

Correspondence should be addressed to Tao Li; litao5555@126.com

Received 29 August 2022; Accepted 7 October 2022; Published 10 November 2022

Academic Editor: Pengfei Wang

In order to explore the dynamic evolution of overburden rock movement and mining-induced stress of an ultra-high working face, taking the ultra-high working face of a 2# thick coal seam in a shallow mine field as the engineering background, this paper analyzes the distribution characteristics of principal stress, mining stress evolution characteristics, overburden rock migration characteristics, and overburden rock caving characteristics of a shallow overburden rock ultra-high working face under different advancing distances and calculates by FLAC^{3D} numerical simulation software. The results show that when the working face advances to 200 m, the stress concentration degree presents a stable trend. The concentration degree and variation gradient of the maximum principal stress are greater than those of the minimum principal stress, while the range of the peak ahead coal wall is smaller than that of the minimum principal stress peak leading coal wall. With the increase of the advancing range, the stress recovery degree gradually increases, and the maximum principal stress recovery degree is higher than the minimum principal stress. When the working face advances to 300 m, the maximum principal stress restores to 66% of the initial value, while the minimum principal stress is only restored to about 50%, and the surface subsidence degree reaches 2.5 m.

1. Introduction

China is both a major country in terms of coal consumption and coal imports. Coal plays an irreplaceable role in the country's economic construction and long-term development. The total monthly import of coal in 2019–2021 is shown in Figure 1. Since 2022, affected by the international environment, the domestic coal price has stayed high. Many countries have begun to participate in the rush to purchase and stockpile coal resources, leading to an insufficient supply of coal capacity, soaring prices, and an increasingly tempestuous relationship between coal supply and demand. Increasing production and ensuring supply is one of the most effective ways to alleviate the tension between supply and demand for coal, and improving the coal recovery rate is an important decision that cannot be ignored [1–4]. According to the relevant policy requirements, the recovery rate of the mining area shall meet the requirements that the thick coal seam is not less than 75%, the medium thick coal seam is not less than 80%, and the thin coal seam is not less than 85% [5–7]. It can be seen that the greater the thickness of the coal seam, the lower the coal recovery efficiency, and a large number of coal resources are subject to mining technology or equipment and other factors that cannot be solved and eventually abandoned. With the increasing depletion of coal resources in mining areas in eastern China, the focus of coal resource development is gradually shifting from the east to the west. The main characteristics of coal seam occurrence in the western region are shallow, thick coal seams, large dip angles, and a wide distribution of thick and extra-thick coal seams (above 8 m) [8–10]. Therefore, improving the recovery rate of shallow and extra-thick coal seams in the western region is the primary issue to be solved urgently.

With the progress of modern science and technology, equipment automation, equipment intelligence, and other aspects are constantly developing, and China's coal mining technology has also entered a stage of rapid development.

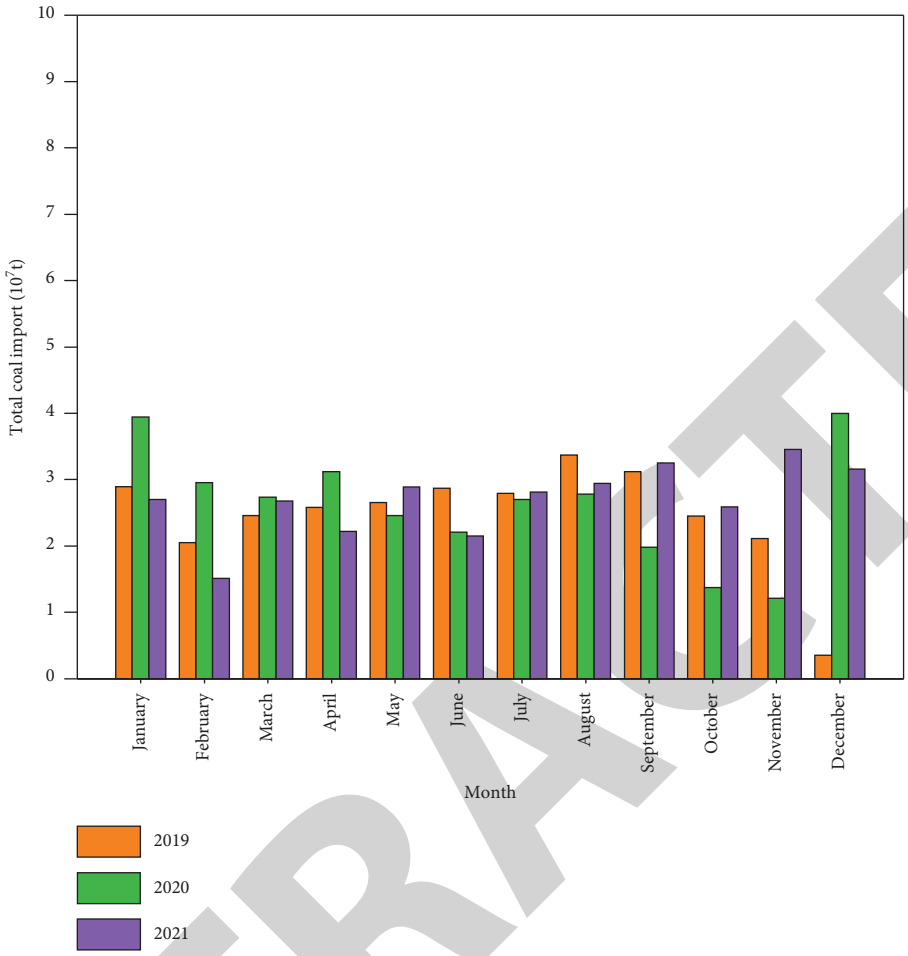

Figure 1: China's total monthly coal imports from 2019–2021.

The application of comprehensive mechanized coal mining technology with large mining height is extremely important in improving coal recovery rates and management levels [11–14]. With the advantages of high recovery rate, high safety, and low tunneling rate, ultra-high working face has been widely used in mining areas in western China and has gradually become the main choice for mining thick coal seams below 8.0 m [15–18]. However, the western mining area also has a large number of extra-thick coal seams with a thickness of 8~15 m and an average thickness of 8 m, which are more difficult to mine, mainly reflected in the large underground space of the stope, the increased difficulty of roof control, and the serious damage of high coal wall damage in the ultra-high working face [19–21]. The larger the mining height, the larger the plastic damage range of the coal wall, and the more serious the damage to the coal wall. The falling coal easily crushes the scraper conveyor and injures the operators. At the same time, it will also induce local roof fall on the end face, which seriously threatens the safety of operators and equipment. Scholars at home and abroad have done a lot of research on the mechanism of rib spalling. MahdevariandMoarefvand proposed that the hardness of coal was the biggest influencing factor on rib spalling [22–24]. Zhao et al. proposed that under the influence of self-weight and roof pressure, the coal wall was mainly in the form of tension failure and shear failure, and a method to determine the support working resistance based on the control of the roof and coal wall was given [25–27]. Chen et al. found through the compressive strength test that when the layering was developed, and there were many weak planes in the coal seam, the coal seam with a low hardness coefficient was more likely to lead to rib spalling, and the flexible reinforcement technology for the prevention and control of ultra-high rib spalling was proposed [1, 28, 29].

With the change of mining range, the movement characteristics of overburden rock and mining stress distribution of shallow buried ultra-high working faces are continuously changing, and the surrounding rock control criteria of ultra-thick coal seam stope should also change appropriately with the change of working face advancing stage. By using the FLAC^{3D} numerical simulation method, this paper researches the overburden rock movement and mining stress distribution during the advancing process of the 2$^{\#}$ main mining ultra-thick coal seam working face in a

mine field, and the overburden rock movement law and mining stress dynamic evolution process of the ultra-high working face were obtained.

2. The Engineering Background and Numerical Model

2.1. The Engineering Background. The basic structural form of a mine field is a monoclinic structure, with a strike of N25° W, a dip of S65° W, and a dip of 1 ~ 3°. The local rock surface is small, and the width is not large, and the maximum is about 5 m. The mine field belongs to a simple structure. There are five coal seams in the mine, with a total thickness of 16.5 m. There are 3 main coal seams with a total thickness of 13.95 m. Among them, the buried depth of the 2# coal seam is 89 ~ 236 m, the thickness of the coal seam is 7.96 ~ 9.26 m, with an average of 8.8 m, which is ultra-thick, and the dip angle of the coal seam is 1 ~ 3°. The relative content of coal seam gas is 0.00013 m3/t and the spontaneous combustion period of coal seam is about 40–60 days. The explosion index of coal dust in the coal seam is 30.50%, which is stable and suitable for large mining height mining technology.

The false roof of the ultra-high working face in the 2# extra thick coal seam is mudstone, with a compressive strength of about 11.3 ~ 13.2 MPa and a Platts coefficient of about 1.32, which is of low firmness and belongs to the unstable type; The immediate roof is gray-white fine-grained sandstone, with a compressive strength of about 13.3 ~ 15.2 MPa and a Platts coefficient of about 1.35. It is strong and belongs to hard unstable type; The main roof is gray white siltstone with the compressive strength of about 14.5 ~ 36.6mpa and the Platts coefficient of about 2.32; The immediate bottom is black gray mudstone, with the compressive strength of about 14.5~29.6mpa and the Platts coefficient of about 2.32. The physical and mechanical parameters of each coal and rock are shown in Table 1. The surface area is largely covered by aeolian sand, resulting in the loose layer thickness of the working face reaching 0~25 m, which causes unconformable contact with the bedrock of the lower working face. The thickness of the bedrock of the working face can reach 52~246 m, due to the thick coal seam with weak cementation and overlying rock. There is a lime ditch on the surface of the working face, and the cutting project is relatively simple with good drainage conditions and general water yield performance.

2.2. Numerical Model. The numerical model is established according to the roof and floor conditions of the ultra-high working face in the 2# main mining extra thick coal seam. As shown in Figure 2, the length and width of the model are 800 m and 400 m, respectively, and the height of the model varies according to the thickness of the bedrock and the overlying loose layer. The simulated working face is 300 m long, and the mining height is 8.8 m. According to the magnitude and direction of in-situ stress measured in the engineering background, the maximum principal stress σ_1 of rock mass in the numerical model stratum is determined to be distributed vertically along the Z axis, and the minimum principal stress σ_3 of the original rock is distributed horizontally along the X axis. During the simulation process, the unit body with broken overburden rock is set as an empty grid to simulate the process of overburden rock collapse, fill the goaf according to the estimated coefficient of overburden rock swelling, and simulate the stress recovery phenomenon in the goaf caused by overburden rock movement. In the simulation process, the coal and rock adopt the Moore–Coulomb constitutive model, and the physical and mechanical parameters of coal and rock are assigned according to Table 1.

3. Analysis of Mining-Induced Stress Distribution and Evolution Characteristics

3.1. Distribution Characteristics of Principal Stress. According to the engineering background, the surface topography is high in the west and low in the east, so the distribution law of the maximum principal stress of the in-situ rock is also high in the west and low in the east in the coal seam, and the surface topography reaches its minimum in the southeast corner. The maximum principal stress of in-situ rock σ_1 is distributed along the coordinate axis Z axis (plumb direction). Affected by the coal seam excavation, the magnitude and direction of the maximum principal stress of each rock stratum will change. The distribution characteristics of the maximum principal stress of the coal seam under different advancing distances are shown in Figure 3 [30]. With the continuous advance of the working face, the classic law of first increasing and then decreasing the in-situ rock stress is formed in the front, rear, and both sides of the goaf. The maximum principal stress far away from the working face shows a high in the west and a low in the east trend and reaches its minimum value in the southeast corner, which is consistent with the distribution law of surface fluctuation. In other words, the higher the surface, the greater the depth, and the greater the maximum principal stress. The stress concentration factor refers to the ratio of the stress at a certain place after the excavation of the coal seam to the stress in the in-situ rock under the state of no excavation. The stress concentration phenomenon refers to the fact that the stress concentration factor at a certain place in the stratum is significantly larger than that in other parts. In general, the stress concentration factor mainly appears in front of the coal wall of the working face, and the stress concentration degree in the middle of the working face and the corners at both ends is relatively large. With the advance of the working face, the maximum principal stress concentration in the middle of the working face is greater than that in the corners at both ends, and the stress concentration in the upper corner is greater than that in the lower corner (the terrain of the upper corner is higher than that of the lower corner, indicating that the greater the buried depth, the greater the stress concentration). On the whole, the stress concentration in front of the work is greater than that behind the goaf, and the stress concentration above the goaf is greater than that below the goaf.

Table 1: Physical and mechanical parameters of coal and rock.

Name	Elastic Modulus (GPa)	Poisson's ratio	Tensile strength (MPa)	Compressive strength (MPa)
Main roof	30.943	0.27	7.14	25.55
Immediate roof	40.313	0.23	6.28	14.25
Coal	23.872	0.25	2.1	11.68
Floor	47.350	0.22	6.77	22.05

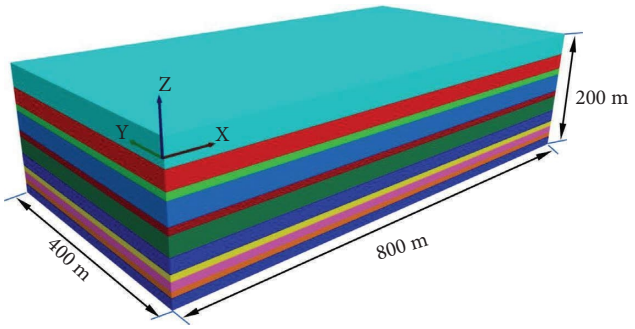

Figure 2: Numerical model.

With the advancement of the working face, the goaf will be gradually filled with gangue and roof subsidence until compaction. At this time, with the filling, the stress in the goaf gradually returns to the in-situ rock stress level, and the greater the advance distance of the working face induce the more sufficient the compaction and the greater the stress recovery value. It can be seen from the figure that with the advance of the working face, the stress recovery degree of the goaf becomes more and more obvious, and the maximum recovery first occurs in the middle of the goaf near the rear, that is, near the middle of the open off cut, and then with the advance of the working face, the maximum recovery value will gradually move in the advancing direction. This phenomenon indicates that although the goaf is filled and compacted section by section, it will affect each other as a whole. The maximum value is biased towards the overall center of the goaf. After the advancing distance of the working face reaches a certain stage, the recovery degree of the goaf is close to the increase of radiation from the inside to the outside of the circle superposition. In the process of advancing the general working face, the influence range of mining is generally 5% greater than the in-situ rock stress as the limit. With the advancing of the working face, the influence range of mining will gradually increase. It can be seen from the figure that with the increase of the advancing distance of the working face, the mining influence range of the maximum principal stress of the coal seam will gradually increase, and it is most obvious in front of the coal wall of the working face, and the change of the influence range behind the goaf will change slightly with the advancing progress. However, when the advancing distance reaches a certain value, the mining influence range will tend to be stable and will not increase. With the increase of the suspension width of the roof in the goaf, the roof in the goaf, especially the main roof, will be broken periodically. With the fracture of the main roof, it is bound to be accompanied by the release of energy, which is reflected in the reduction of stress concentration in terms of stress, the increase in stress recovery in the goaf, and the reduction of the influence range in terms of the influence range of mining. With the main roof fracture, the stress concentration degree of the coal seam decreases, the stress recovery degree of the goaf increases, and the influence range of mining decreases.

According to the model, the minimum principal stress of the in-situ rock $\sigma 3$. Distributed along the x-axis and affected by the undulating characteristics of the surface topography in the West and East, the minimum principal stress of the in-situ rock of the model is large in the west and small in the east. After the coal seam is excavated, the minimum principal stress and stress concentration value near the coal seam in front of the working face are bound to change. Due to the main roof caving filling of the goaf behind the working face, the minimum principal stress is restored, while it is far less than the original values. With the continuous advance of the working face, the stress concentration phenomenon appears above the coal wall and around the goaf. When the main roof is broken, the stress concentration phenomenon above the coal wall is weakened, the stress concentration value and influence range are reduced, and the stress concentration phenomenon around the goaf changes little. The distribution characteristics of the minimum principal stress under different propulsion distances are shown in Figure 4 [30].

The initial stress concentration value of coal seam mining is small, which increases by about 16.67% compared with the initial in-situ rock stress. When the advance is 32 m, the influence range of stress concentration is about 75 m ahead of the coal wall. With the advance of the working face, the influence range increases gradually, but the increase in speed slows down, and the influence range is stable at about 100 m in front of the coal wall in the later stage. When the advancing distance reaches 96 m, the minimum principal stress reaches 2.75 MPa, which is 2.2 times the initial in-situ rock stress. When the advancing distance reaches 224 m, the minimum principal stress is 3.25 MPa, which is 2.6 times the initial in-situ rock stress. As the working face continues to advance, when the advancing distance reaches 352 m, the stress concentration value drops back to 2.75 MPa. The stress concentration range on both sides of the goaf increases continuously. When the working face advances to 192 m, the stress concentration value increases nearly twice. The stress concentration value on the north side of the goaf is higher than that on the south side, about 0.05 MPa higher. The stress concentration phenomenon is symmetrically distributed from the middle of the goaf to the front and back, and its distribution characteristics can be seen to be weakly affected by the surface topography.

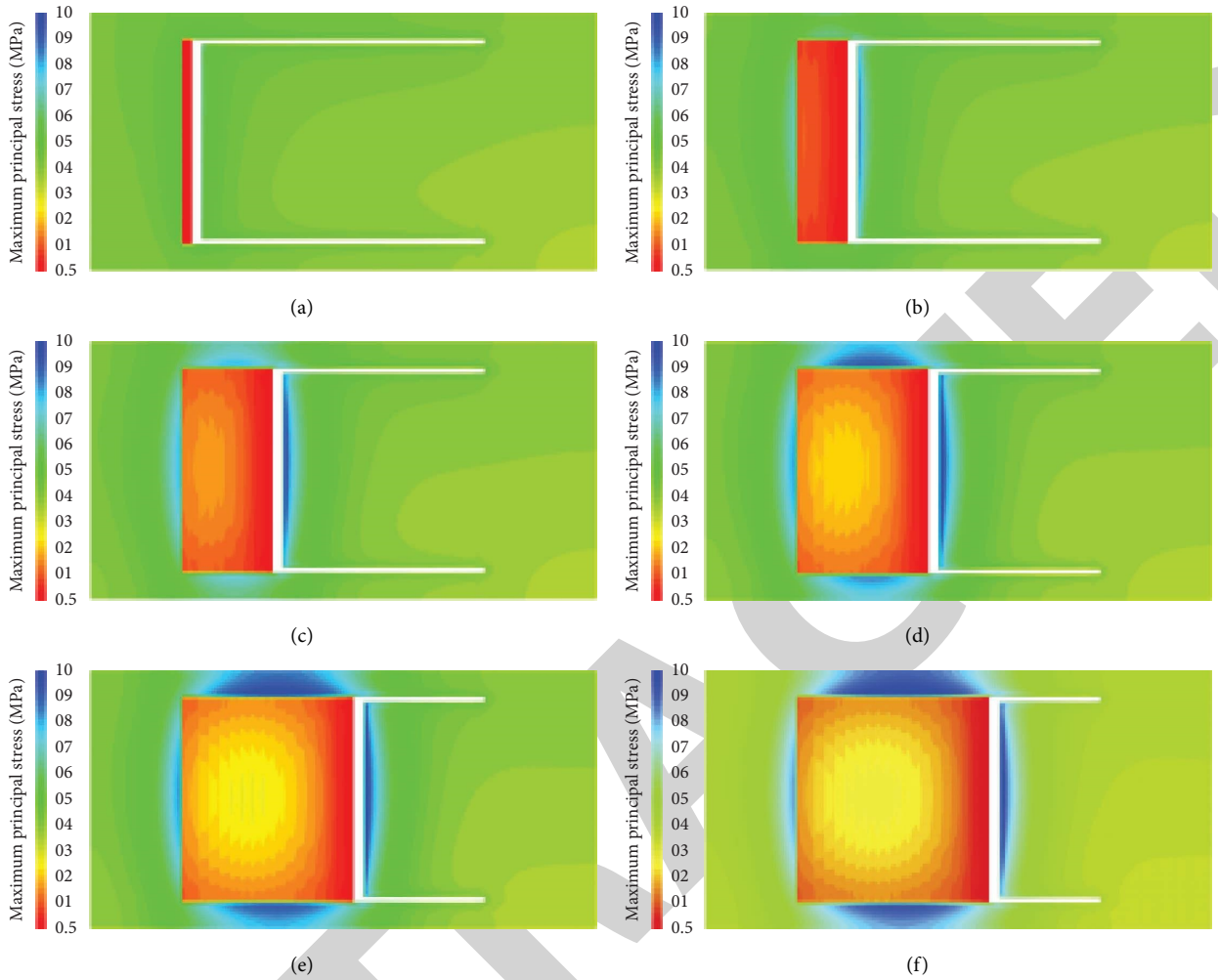

Figure 3: Distribution characteristics of maximum principal stress under different propulsion distances: (a) advance 32 m, (b) advance 96 m, (c) advance 160 m, (d) advance 224 m, (e) advance 288 m, and (f) advance 352 m.

After the coal seam is mined out, a goaf forms. The pressure is released rapidly, and the stress is eliminated. With the immediate roof caving, the main roof will bend and sink, and the goaf will be filled again. The collapsed immediate roof will fill the goaf and connect with the main roof. At this time, the stress will reappear, and the stress will gradually recover from the back of the goaf to the working face as the working face advances. When the advance reaches 96 m, the stress within 40 m behind the goaf gradually begins to recover. At this time, the minimum principal stress is about 0.25 MPa, which is about 20% of the initial in-situ rock stress. The stress recovery value is elliptic in the middle of the gob enrichment area, radiating and decreasing to the four sides. The inclination direction is the long axis of the ellipse, and the strike direction is the short axis of the ellipse. When the working face advances to 256 m, the stress recovery value of the goaf reaches 0.75 MPa, which is about 60% of the initial value. With the working face advancing to 352 m, the stress recovery area increases, but its recovery value does not change.

Compared to the stress distribution before and after the breaking of the main roof at different advance distances, it can be seen that after the breaking of the main roof, the value of stress concentration near the coal wall is significantly reduced, and the influence range of stress concentration is narrowed. Especially after the advance distance reaches 160 m, the weakening effect of the breaking of the main roof on the stress concentration above the coal wall is particularly prominent. After the main roof collapsed, the stress concentration value in front of the coal wall decreased from 3.25 MPa to 2.5 MPa, down nearly a quarter. The breaking of the main roof has a weak influence on the stress concentration on both sides of the goaf and promotes the compaction of the middle and rear of the goaf.

In summary, with the continuous advance of the working face, there will be obvious stress concentration in front of the coal wall, but the stress concentration at the coal wall will weaken after the square. The main roof breaking can alleviate the stress concentration in front of the coal wall. Therefore, strengthening roof management, timely roof caving, and pressure relief play an important role in the safety of the working face.

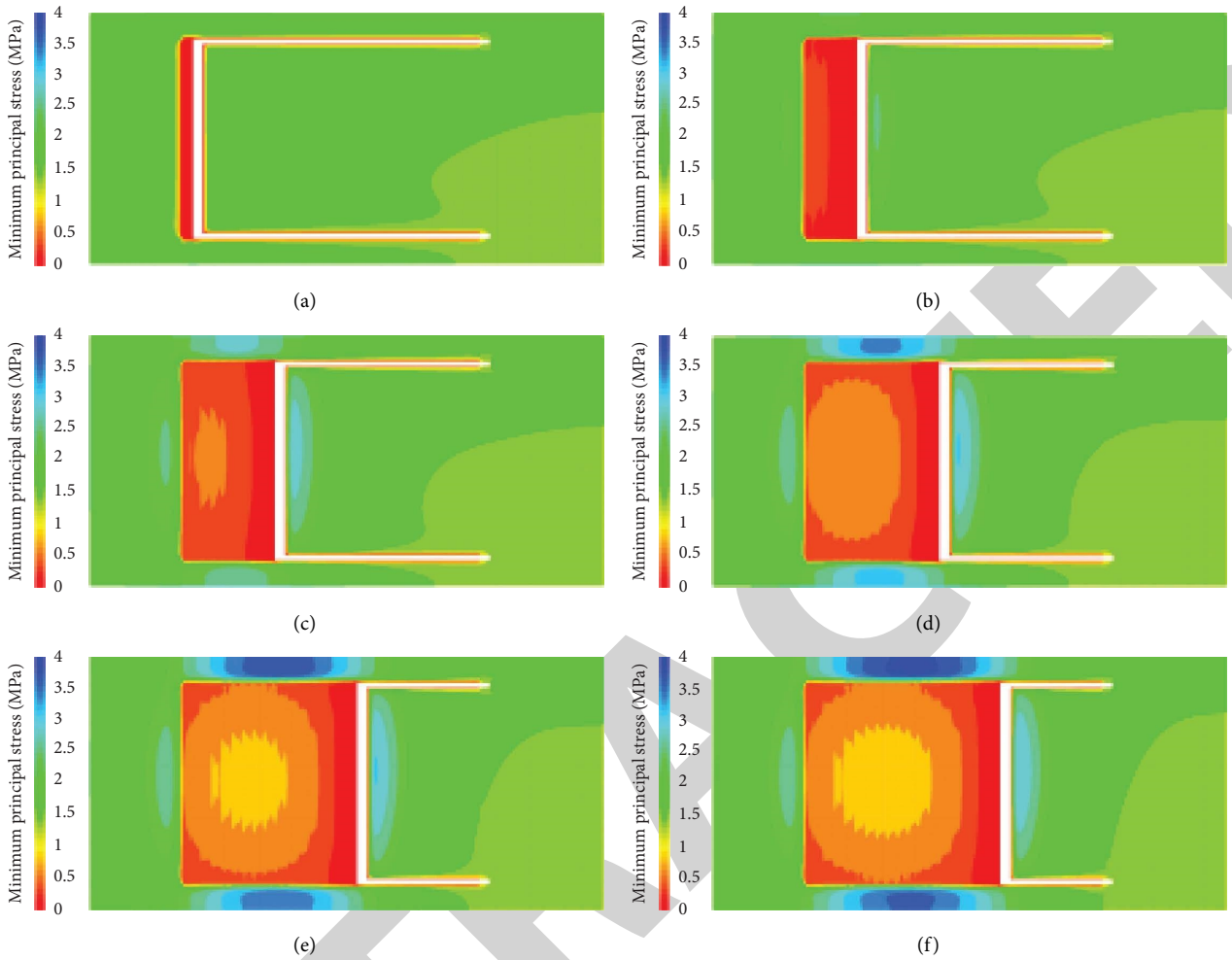

Figure 4: Distribution characteristics of minimum principal stress under different propulsion distances: (a) advance 32 m, (b) advance 96 m, (c) advance 160 m, (d) advance 224 m, (e) advance 228 m, and (f) advance 352 m.

3.2. Evolution Characteristics of Mining-Induced Stress. During the advancing process of the working face, the stress evolution characteristics of the solid coal in front of the coal wall and the goaf behind are shown in Figure 5. After the coal seam is mined, the gravity of the overlying rock above the goaf transfers to the surrounding solid coal, resulting in an increase in the maximum and minimum principal stresses in the solid coal. In the initial mining stage, the maximum and minimum principal stress concentrations are low. With the increase of the advancing range of the working face, the maximum and minimum principal stress concentrations gradually increase. When the working face advances to 200 m per month, the maximum and minimum principal stress concentrations are basically stable. With the increase of the advancing range of the working face, the maximum and minimum principal stresses in the goaf behind the working face show a gradual recovery phenomenon. The larger the mining range, the more sufficient the movement of the overlying strata and the higher the recovery degree of the maximum and minimum principal stresses in the goaf. When the working face advances to 300 m, the maximum principal stress recovers to 2.8 MPa, about 66% of the in-situ rock stress value, and the minimum principal stress recovers to 0.8 MPa, about 50% of the in-situ rock stress value.

When comparing the evolution characteristics of the maximum and minimum principal stresses, it can be seen that in the solid coal in front of the working face, the concentration degree and variation gradient of the maximum principal stress are significantly greater than the minimum principal stress, and at the same time, the recovery degree of the maximum principal stress in the goaf behind the working face is also greater than the minimum principal stress. The distance of the maximum principal stress peak ahead of the coal wall is significantly less than that of the minimum principal stress peak ahead of the coal wall, indicating that the redistribution range of the minimum principal stress caused by mining is larger. In addition, the breaking of the main roof has a significant impact on the concentration degree of mining stress. After the breaking of the main roof, the peak value of the maximum and minimum principal stress suddenly decreases, which indicates that the violent movement of overlying rock will cause the sudden release of mining stress in front of the working face.

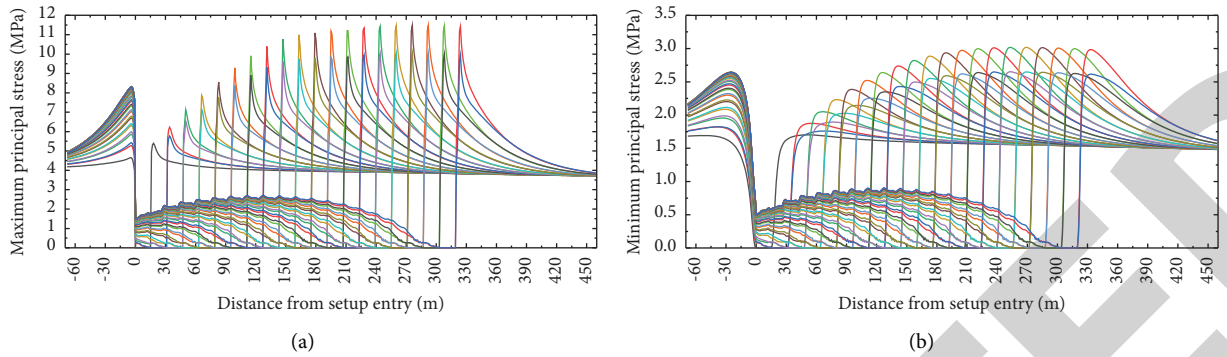

Figure 5: Evolution characteristics of principal stress during mining, (a) maximum principal stress, (b) minimum principal stress.

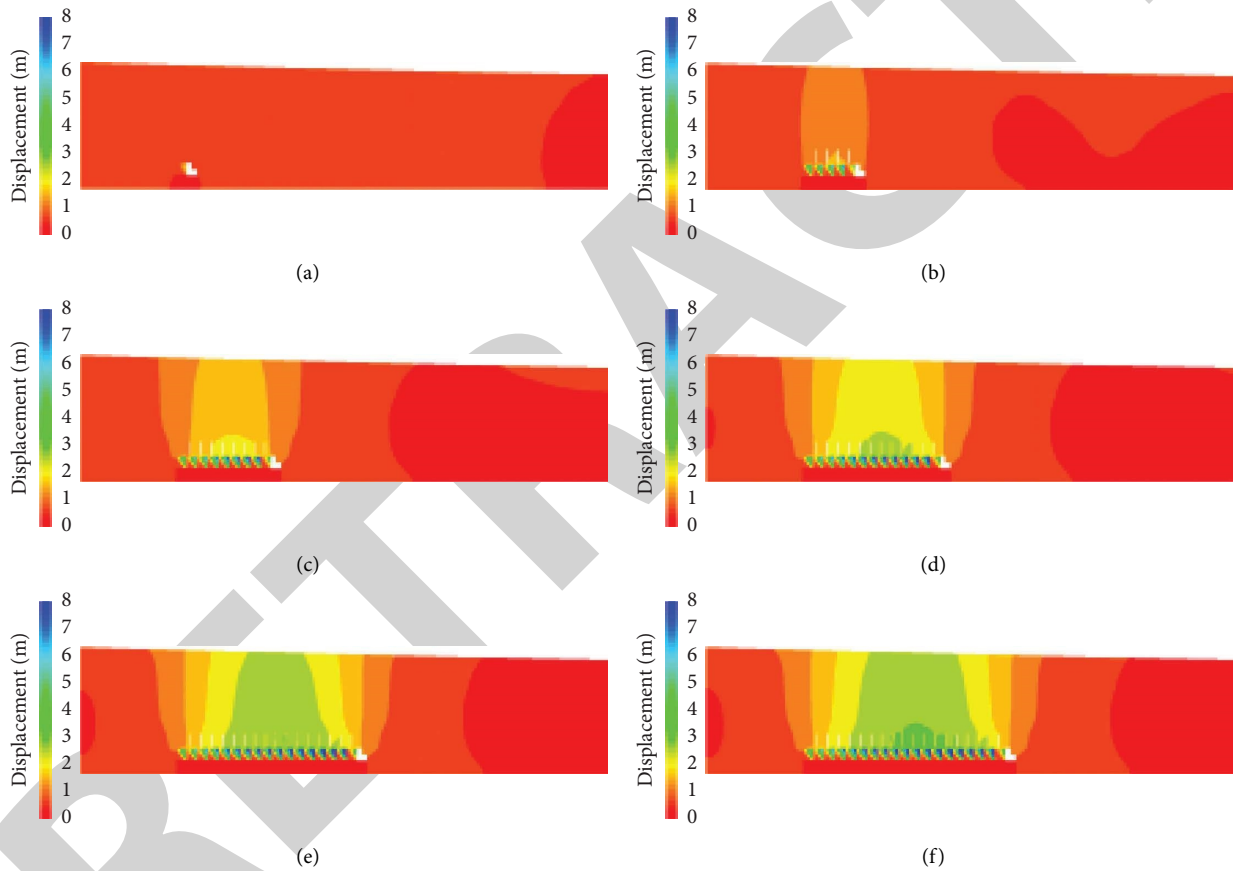

Figure 6: Overlying rock migration characteristics of ultra-high working face under different advancing distances: (a) advance 32 m, (b) advance 96 m, (c) advance 160 m, (d) advance 224 m, (e) advance 288 m, and (f) advance 352 m.

4. Overburden Rock Movement Law of Ultra-high Working Face

4.1. Characteristics of Overburden Rock Movement. The migration characteristics of overburden rock under different advancing distances of ultra-high working faces are shown in Figure 6 [30]. Cloud images of vertical displacement of overburden rock at each stage of the working face from open off cut to 352 m in advance. With the mining of coal seams, when the working face advances 32 m, the roof at the open off cut has obvious vertical displacement, and the vertical displacement reaches 2.10 m. As the working face advances to 96 m, the roof subsidence reaches 4.00 m. At this time, the main roof of the working face has broken, and the vertical displacement of the roof has increased rapidly. When the working face advances to 160 m, the roof subsidence reaches 4.50 m, the roof subsidence trend gradually tends to be stable, and the roof subsidence gradually develops to the surface. With the working face advancing to 224 m, after the second periodic weighting of the main roof, the height of the roof falling zone increased significantly, the surface subsidence area increased significantly, and the roof subsidence

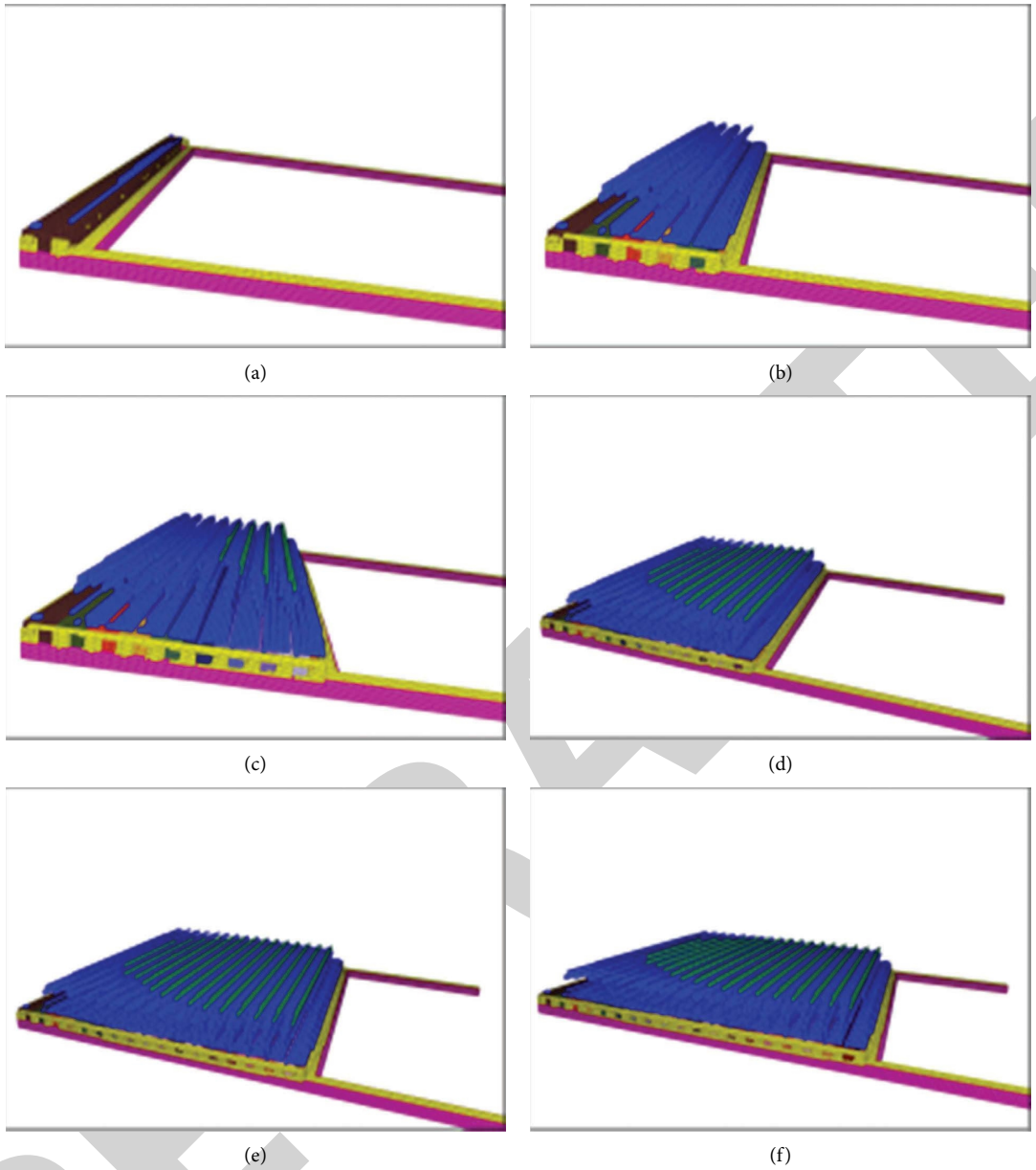

Figure 7: Overburden rock caving characteristics of ultra-high working face under different advancing distances: (a) advance 32 m, (b) advance 96 m, (c) advance 160 m, (d) advance 224 m, (e) advance 288 m, and (f) advance 352 m.

tended to be stable at 5.50 m. When the working face advances to 288 m, the maximum roof subsidence gradually extends to the surface, the surface subsidence area increases significantly, and the roof subsidence tends to be stable at 5.50 m. With the working face advancing to 352 m, a subsidence basin appeared on the surface, and the subsidence reached 4.40 m, and the roof subsidence of the working face reached 6.0 m.

4.2. Characteristics of Overburden Rock Caving. The whole process of overburden rock collapse of a shallow ultra-high working face is characterized by numerical simulation of the range of plastic failure zone. The overburden rock collapse characteristics of an ultra-high working face under different advancing distances are shown in Figure 7. When the working face advances to 32 m, the main roof is pressed for the first time. Due to the small mining range, the disturbance degree of overlying rock is low, and the collapse range of overlying rock is small, including only the immediate roof, the main roof, and a small amount of follow-up rock above it. The caving height is about 15 m. When the advancing range of the working face increases to 96 m due to the increase in the mining range, the range of the caving roof increases both vertically and horizontally, and the caving height increases to 35 m. When the advancing range of the working face is between 96 m and 160 m, the roof caving range basically remains unchanged in the longitudinal direction and only expands laterally in the advancing direction of the working face. This is because

the main roof controls the movement of overlying strata as the first key layer. At this stage, the second key stratum layer above the main roof is still not damaged, and the second key stratum layer controls the strata above it to ensure that the upper strata do not collapse. Therefore, the collapse range at this stage does not change in the longitudinal direction. The collapsed overburden rock is only the following strata between the main roof and the second key stratum layer. When the working face advances to 224 m, the second key stratum layer in the overburden rock is broken, the caving range of the overburden rock increases longitudinally, and the caving height increases to 43 m. Since then, the collapsed overburden rock has completely filled the goaf due to the crushing and swelling phenomenon, which has a supporting effect on the upper strata, and the collapse range of the overburden rock has no longer changed. With the movement of the upper strata, the collapsed gangue that is gradually compacted results in the stress recovery phenomenon in the goaf.

5. Conclusions

(1) The simulation results of the overburden rock movement characteristics in the process of advancing show the maximum and minimum principal stresses in the coal seam appear in front of the working face, and the degree of stress concentration increases with the increase of the advancing range of the working face. When the working face advances to 200 m, the degree of stress concentration shows stable characteristics. The concentration degree and variation gradient of the maximum principal stress are greater than those of the minimum principal stress, while the peak ahead coal wall range is less than that of the minimum principal stress peak ahead coal wall range.

(2) The stress recovery phenomenon occurred in the goaf. With the increase of the working face advancing range, the stress recovery degree gradually increased, and the maximum principal stress recovery degree was higher than the minimum principal stress. When the working face advanced to 300 m, the maximum principal stress recovered to 66% of the initial value, while the minimum principal stress only recovered to about 50%.

(3) The evolution characteristics of overburden rock movement and surface subsidence with the advance of the working face are obtained. The results show that when the working face advances to 300 m, the degree of surface subsidence reaches 2.5 m, which is consistent with the measured results, verifying the accuracy of the numerical calculation results.

Data Availability

The datasets generated during and/or analysed during the current study are available from the corresponding author on reasonable request. All data generated or analysed during this study are included in this published article. Some of the data analysed during this study is properly cited in the manuscript and referenced in the References section.

Conflicts of Interest

The authors declare that they have no conflicts of interest.

Acknowledgments

This work was financially supported by the Joint Guiding Project of Natural Science Foundation of Heilongjiang (grant no. LH2019E118) and the Basic Scientific Research Funds of Heilongjiang Provincial Undergraduate Institutions (grant no. 2021-KYYWF-1171).

References

[1] J. H. Chen, P. Liu, L. Liu et al., "Anchorage performance of a modified cable anchor subjected to different joint opening conditions," *Construction and Building Materials*, vol. 336, pp. 127558–127612, 2022.

[2] J. Gao and H. T. He, "Application of fully mechanized full seam one passing mining technology to thick seam in Shendong mining area," *Journal of China Coal Society*, vol. 35, pp. 1888–1892, 2022.

[3] H. J. Wang, "Technology study of fully mechanized working face over 8 m of shendong coal mine," *Coal Technology*, vol. 33, pp. 169–171, 2014.

[4] L. H. Zhang and N. N. Li, "Study on ground pressure behavior law of 8m super high fully mechanized mining face," *Coal Science and Technology*, vol. 45, pp. 21–26, 2017.

[5] S. Di, J. J. Wang, and G. J. Song, "Study on rib spalling characteristics of 8.5m height fully mechanized mining face," *Coal Science and Technology*, vol. 45, pp. 97–102, 2017.

[6] J. Z. Yang, "Study on overlying strata breakage and strata behaviors law of 7.0 m mining height working face," *Coal Science and Technology*, vol. 45, pp. 1–7, 2017.

[7] Z. Q. Song, S. K. Liang, and J. Q. Tang, "Study on the influencing factors of coal wall rib spalling in fully mechanized working face," *Journal of Hunan University of Science &Technology (Social Science Edition)*, vol. 26, pp. 1–4, 2011.

[8] J. C. Wang, "Rib spalling and prevention mechanism in extremely soft thick coal seams," *Journal of coal*, vol. 75, pp. 785–788, 2007.

[9] J. C. Wang, L. Wang, and Y. Guo, "Determination of working resistance based on roof and coal wall control," *Journal of coal*, vol. 39, pp. 1619–1624, 2014.

[10] J. C. Wang, S. L. Yang, and D. Z. Kong, "Failure mechanism and control technology of longwall coal face in large-cutting-height mining method," *International Journal of Mining Science and Technology*, vol. 26, pp. 111–118, 2016.

[11] S. L. Yang and D. Z. Kong, "Mechanism and application of flexible reinforcement for prevention and control of super high coal wall slope," *Journal of coal*, vol. 40, pp. 1361–1367, 2015.

[12] S. L. Yang, D. Z. Kong, and J. H. Yang, "Coal wall stability and grouting reinforcement technique in fully mechanized caving face during topple mining," *Journal of Mining & Safety Engineering*, vol. 35, pp. 827–833+839, 2015.

[13] L. Chen, X. R. Meng, and Z. N. Gao, "Analysis on spalling mechamism of coal wall law for fully mechanized high cutting

coal mining face," *Coal Science and Technology*, vol. 39, pp. 18–20+24, 2011.
[14] J. F. Ju and J. L. Xu, "Structural characteristics of key strata and strata behaviour of a fully mechanized longwall face with 7.0 m height chocks," *International Journal of Rock Mech anics and Mining Sciences*, vol. 58, pp. 46–54, 2013.
[15] J. H. Wang, "New development of rock bolting technology for coal roadway in China," *Journal of China Coal Society*, vol. 32, pp. 113–118, 2007.
[16] Y. D. Jiang, Y. X. Zhao, and W. G. Liu, "Research on floor heave of roadway in deep mining," *Chinese Journal of Rock Mechanics and Engineering*, vol. 23, pp. 2396–2401, 2004.
[17] G. A. Covic and J. T. Boys, "Modern trends in inductive power transfer for transportation applications," *IEEE Journal of Emerging and Selected Topics in Power Electronics*, vol. 1, pp. 28–41, 2013.
[18] H. P. Xie, G. M. Yu, and L. Yang, "Research on the fractal effects of crack network in overburden rock rock stratum," *Chinese Journal of Rock Mechanics and Engineering*, vol. 18, pp. 147–151, 1999.
[19] Z. G. Wang, H. W. Zhou, and H. P. Xie, "Research on fractal characterization of mined crack network evolution in overburden rock rock stratum under deep mining," *Rock and Soil Mechanics*, vol. 30, pp. 2403–2408, 2009.
[20] D. Huang, Q. Tan, and R. Q. Huang, "Fractal characteristics of fragmentation and correlation with energy of marble under unloading with high confining pressure," *Chinese Journal of Rock Mechanics and Engineering*, vol. 31, pp. 1379–1389, 2012.
[21] K. Zhang, Y. L. Chen, W. C. Fan, X. Liu, H. Luan, and J. Xie, "Influence of intermittent artificial crack density on shear fracturing and fractal behavior of rock bridges: experimental and numerical studies," *Rock Mechanics and Rock Engineering*, vol. 53, no. 2, pp. 553–568, 2020.
[22] S. Mahdevari and P. Moarefvand, "Experimental investigation of fractal dimension effect on deformation modulus of an artificial bimrock," *Bulletin of Engineering Geology and the Environment*, vol. 77, no. 4, pp. 1729–1737, 2018.
[23] F. Y. Liu, T. H. Yang, and P. H. Zhang, "Dynamic inversion of rock fracturing stress field based on acoustic emission," *Rock and Soil Mechanics*, vol. 39, pp. 1517–1524, 2018.
[24] D. Duan, Y. Zhao, and R. Z. Zhang, "Acoustic emission characterization of uniaxial compression failure characteristics of mudstone based on Micro-CT," *Journal of Vibration and Shock*, vol. 39, pp. 163–170, 2020.
[25] X. D. Zhao, Y. H. Li, and R. P. Yuan, "Study on crack dynamic propagation process of rock samples based on acoustic emission location," *Chinese Journal of Rock Mechanics and Engineering*, vol. 26, pp. 944–950, 2007.
[26] J. Liu, E. Y. Wang, and D. Z. Song, "Effects of rock strength on mechanical behavior and acoustic emission characteristics of samples composed of coal and rock," *Journal of China Coal Society*, vol. 39, pp. 685–691, 2014.
[27] Q. Sun, W. Q. Zhang, and L. Xue, "Acoustic emission characteristics in quasi-quiet stage of damage and fracture of sandstone," *Jou Min Safe Eng*, vol. 30, pp. 237–242, 2013.
[28] J. H. Chen, B. Q. Zeng, L. Liu et al., "Investigating the anchorage performance of full-grouted anchor bolts with a modified numerical simulation method," *Engineering Failure Analysis*, vol. 141, pp. 106640–106714, 2022.
[29] T. Li, H. Gong, and G. L. Xu, "Study on the influence of in situ stress distribution on the stability of roadway surrounding rock," *Advances in Civil Engineering*, vol. 2021, pp. 1–11, Article ID 3570523, 2021.
[30] Y. J. Liu, H. J. Wang, Q. J. Qi, and A. Wang, "Dynamic evolution law of overburden rock in shallow-buried super-high fully mechanized working face and determination of support strength," *Shock and Vibration*, Article ID 7649459, 2021.